0273-2289/90/2425—0521$02.40

Liquid Phase Dehydration of Ethanol Solutions in a Fixed Bed of Molecular Sieves

WAH KOON TEO* AND HWEI CHEN TI

Department of Chemical Engineering, National University of Singapore, Singapore

ABSTRACT

The liquid phase dehydration of ethanol solutions with type 3A molecular sieves in fixed-bed adsorption columns has been studied under ambient conditions. The breakthrough curves for this system are well predicted by the model of Weber and Chakravorti, which considers both the effects of external film and internal pore diffusional resistances. The concept of mass transfer zone (MTZ) provides a simple design procedure for the system. The fraction ability of the adsorbent within the mass transfer zone to adsorb solute was found to have a constant value of 0.43. The MTZ length was observed to be independent of bed height. Variations of MTZ length with feed concentration and fluid velocity were evaluated.

Index Entries: Ethanol dehydration; adsorption; molecular sieves.

Abbreviations Used: C, concentration of sorbate in bulk liquid phase; C_o, initial value of C; D_m, molecular diffusivity; D_p, pore diffusion coefficient (defined on a pore sectional area basis); D_e, effective diffusivity $= \epsilon_p D_p C_o/q_s$; f, fractional ability of adsorbent in MTZ to adsorb solute at the breakthrough point, dimensionless; k_f, external fluid film mass transfer coefficient, cm/s; L_o, length of fixed bed; L_{MTZ}, length of mass transfer zone; MTZ, mass transfer zone or adsorption zone; N_p, dimensionless parameter defined in Eq. (2); N_f, dimensionless film resistance parameter defined in Eq. (3); q_s, saturation adsorbed phase concentrations (particle volume basis); q, adsorbed phase concentration averaged over a particle; Q, fractional approach to equilibrium $= q/q_s = C/C_o$; Q_E, fractional adsorbate concentration at

*Author to whom all correspondence and reprint requests should be addressed.

bed exhaustion, arbitrarily defined at 0.95; Q_B, fractional adsorbate concentration at breakthrough, arbitrarily defined at 0.075; R_p, particle radius; t, time; t_E, exhaustion time of the bed; t_B, breakthrough time; V, fluid velocity in the bed; W_E, quantity of anhydrous ethanol from a fixed-bed adsorber at bed exhaustion; W_B, quantity of anhydrous ethanol from fixed-bed adsorber at the breakthrough point; θ, dimensionless time variable defined in Eq. (4); ϵ_p, porosity of particle; ϵ, voidage of adsorbent bed.

INTRODUCTION

The production of fuel alcohol and chemicals from renewable resources has been of sustained interest. Regardless of the source of ethanol, either from sugar fermentation or direct hydration of ethylene, the crude product is usually a dilute aqueous solution. For fuel alcohol to be blended with gasoline, almost complete separation of ethanol and water is essential. Therefore, the cost of separation and purification is one of the major considerations in fuel ethanol production. The conventional process of separation is by distillation. Because of the formation of a minimum boiling azeotrope, distillation yields only 95 wt% ethanol under normal conditions. Further purification to produce anhydrous ethanol is normally accomplished by azeotropic distillation using a volatile entrainer or extractive distillation employing an extractive solvent. The high costs of these energy-intensive processes have spurred research to develop other nonconventional processes.

Molecular sieves have successfully been employed in many industrial applications for gaseous phase drying and dehumidification operations. In liquid phase dehydration, molecular sieves have also been shown to be effective adsorbents for the removal of water from ethanol. The results of equilibrium adsorption and batch uptake kinetics, including some preliminary fixed-bed data for dehydration using type 3A molecular sieves, have been reported previously (*1*). This paper presents and analyzes the breakthrough curves for fixed-bed dehydration of ethanol solutions under various operating parameters.

METHODS

Material

A type 3A molecular sieve in 1/16-in. cylindrical pellet form (Sigma Chemical Co., St. Louis, MO) was used exclusively in the experimental work. This adsorbent has the advantage of micropores that are small enough to exclude ethanol. This means that the capacity for water is not reduced by the presence of excess ethanol in the liquid phase. The molecular sieve was preconditioned by thermal activation in a furnace maintained

at 300°C for 24 h. The sieve was then stored in a vacuum desiccator for use in adsorption studies. Mixtures of ethanol and water were prepared from deionized water and analytical grade absolute alcohol (0.79 g/l, minimum purity 99.8 wt%) supplied by Merck (Schuchardt Darmstadt, FRG). Industrial grade, rectified alcohol (95 wt%) was also used in fixed-bed studies. Breakthrough experiments were carried out in jacketed glass columns (2.54 cm diameter × 1.0 m height) packed with preconditioned molecular sieve pellets. The column was maintained at 24°C. The feed, an ethanol–water mixture containing a desired concentration of water, was introduced at the bottom. The operating flow rates ranging from 0.0482 to 0.1067 cm/s were well below the terminal settling velocity of the adsorbent particles in the bed. Samples of the effluent from the column were collected at suitable time intervals and analyzed chromatographically for water and ethanol contents to establish the breakthrough curves. A Perkin-Elmer Model F-17 gas chromatograph with a chromosorb-102 column and a hot wire detector was used for the analysis.

RESULTS AND DISCUSSION

Breakthrough Curves in Fixed-Bed Adsorption

Theoretical Predictive Models

Several theoretical models have been proposed to describe fixed-bed adsorption (2). The application of these models depends very much on the shape of the equilibrium curve or form of adsorption isotherm. For the adsorption of water on type 3A molecular sieves, the highly favorable isotherm, shown in Fig. 1, may be seen to be approaching rectangular or irreversible form. For a rectangular isotherm system, in which the mass-transfer rate is controlled predominantly by internal pore diffusion, the breakthrough curves may be predicted by the pore models proposed by Weber and Chakravorti (3) and Cooper and Liberman (4). Both these models picture the particles as consisting of a solid phase interspersed with very small pores. The former takes into account the combined effects of external film and internal pore diffusional resistances, whereas the latter considers only internal pore diffusion. The relevant expression for the dual resistance pore model of Weber and Chakravorti, as applied to the constant pattern regime ($\theta > 5/2 + N_p/N_f$), is given as follows

$$\theta - N_p = (15/\sqrt{3}) \tan^{-1}\{[2(1-Q)^{1/3} + 1]/\sqrt{3}\} - (15/2) \ln[1 + (1-Q)^{1/3} + (1-Q)^{2/3}] + 2.5 - 5\pi/2\sqrt{3} + (N_p/N_f)(\ln Q + 1) \quad (1)$$

where Q is the fractional uptake and within the constant pattern regime is

$$Q = q/q_s = C/C_o$$

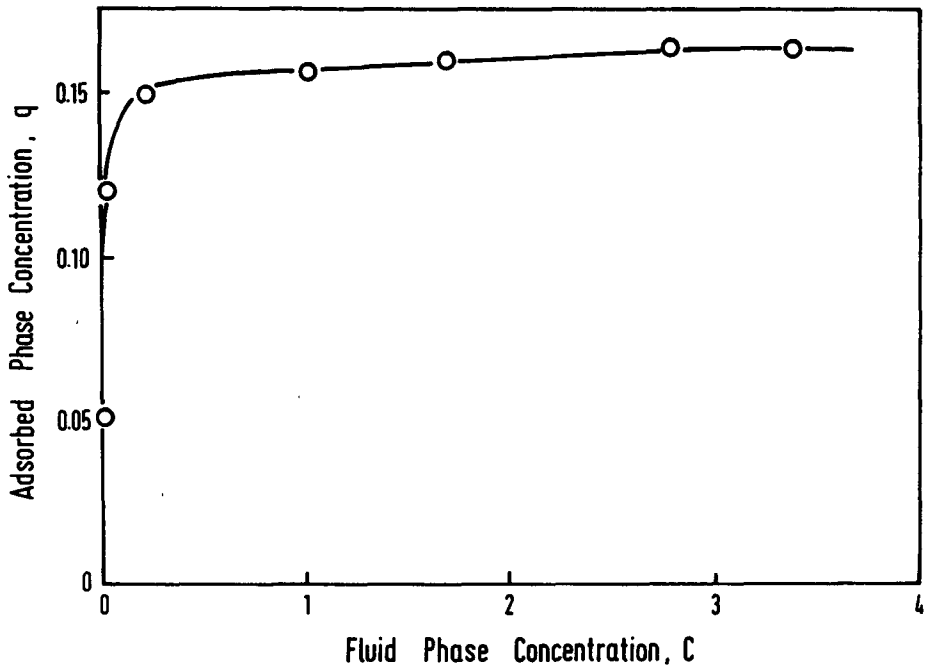

Fig. 1. Adsorption Isotherm at 24°C.

and θ, N_p, and N_f are dimensional parameters with respect to contact time, pore resistance, and film resistance, respectively. These parameters are defined as

$$\theta = (15\,\epsilon_p\,D_p / R_p^2)\,(C_o / q_s)\,(t - L_o / v) \quad (2)$$

$$N_p = (15\,\epsilon_p\,D_p / R_p^2)\,[(1 - \epsilon) / \epsilon]\,(L_o / v) \quad (3)$$

$$N_f = k_f\,[(1 - \epsilon) / \epsilon]\,[3\,L_o / (v\,R_p)] \quad (4)$$

If external mass transfer resistance is negligible ($N_p/N_f \rightarrow 0$). Equation (1) reduces to the expression for a pore diffusion controlled system, given earlier by Cooper and Liberman (*4*).

The equilibrium capacity, q_s, and the diffusional time constant, $\epsilon_p D_p$, have been determined from the batch uptake kinetic studies (*1*), and the external mass transfer coefficient may be estimated from established correlations. Therefore, the dual resistance pore model (Eq. (1)) or the pore diffusion controlled model may be used to describe water adsorption in packed bed of type 3A molecular sieves once the fluid composition, velocity, bed length, and bed voidage are specified.

Mass Transfer Zone (MTZ) Model

A simple approach that has found wide application in the design calculation of adsorption systems is based on the concept of MTZ. The model expresses the total resistance to mass transfer in terms of a length of unused bed or an amount of unused adsorbent that must be added to the

adsorbent equilibrium requirement (*5*). The MTZ concept, originally suggested by Michaels (*6*) for fixed-bed ion-exchange processes, had been developed by Treybal (*7*) and applied to adsorption beds. The height of the MTZ for a given fixed-bed condition has been shown to be (*7*)

$$L_{MTZ} = L_o \{ (t_E - t_B)/[t_E - (1 - f)(t_E - t_B)] \} \quad (5)$$

or, in terms of quantities of water-free ethanol

$$L_{MTZ} = L_o \{ (W_E - W_B)/[W_E - (1 - f)(W_E - W_B)] \} \quad (6)$$

where f, the fractional ability of the adsorbent within the MTZ to still adsorb solute at the breakpoint, is given by

$$f = [\int_{t_B}^{t_E} (Q_o - Q)dt]/[Q_o (t_E - t_B)] \quad (7)$$

The value of f depends on the shape of the breakthrough curve. The MTZ length and f can be determined from the breakthrough curve for a given set of conditions. The fraction approach to saturation of the column at the breakthrough point can be shown as follows

$$\% \text{ Bed saturation} = 100\% [(L_o - fL_{MTZ})/L_o] \quad (8)$$

Therefore, it is possible to predict the height of an adsorber or the quantity of adsorbent needed for a given adsorbate loading.

The MTZ model provides a simple approach to the design calculation of fixed-bed adsorbers. However, the method is limited to isothermal operation from dilute feed mixtures, negligible dispersion and heat effects, and a constant MTZ length that is independent of bed height.

Analysis of Experimental Breakthrough Curves

Breakthrough curves for drying rectified alcohol in packed bed of molecular sieve particles were measured at various flow rates, bed heights, and water contents in alcohol solutions. The results are presented in Figs. 2–4.

Application of the Pore Models

The experimental breakthrough curves are compared with theoretically-predicted curves based on the pore models with and without the consideration of external film resistance as given by Eq. (1). The theoretical curves were calculated using the equilibrium capacity of the sorbate q_s and the diffusional time constant $\epsilon_p D_p/R_p^2$ evaluated from the batch uptake studies (*1*). The external mass transfer coefficients were estimated from the correlation given by Wakao and Funazkri (*8*).

$$Sh = 2k_f R_p / D_m = 2.0 + 1.1\, Sc^{1/3}\, Re^{0.6} \quad (9)$$

The above equation has been shown to provide a good estimation of mass transfer coefficients in fixed-bed operations over a wide range of Reynolds number. The experimental conditions and parameters for calculation of breakthrough curves are summarized in Table 1.

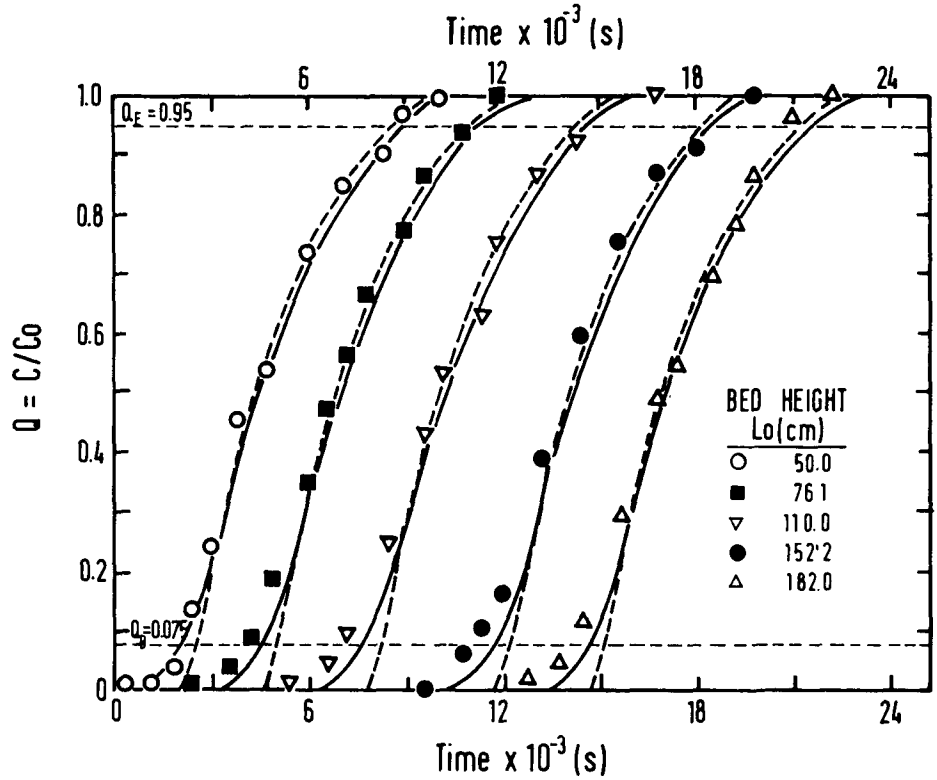

Fig. 2. Breakthrough curves: Effect of bed height. Co = 0.0386 (g/cm³); V = 0.0822 (cm/s); Temp = 24°C. (———): Dual resistance pore model; (– – –): pore model with no external film resistance.

The effect of fixed-bed height at a constant temperature of 24°C, a feed concentration of 0.0386 g/cm³ and a flow rate of 0.0822cm/s is presented in Fig. 2. Comparison of the experimental breakthrough curves for different bed lengths under otherwise identical conditions confirms a constant pattern behavior of the adsorbent–adsorbate system studied.

It is evident from Fig. 2 that generally both the pore models reasonably represent the later portions of the breakthrough curves. The theoretical breakthrough curves calculated from the dual resistance model (i.e., intraparticle diffusion + external film resistance) give a better prediction of the experimentally observed behavior in the initial region. In this region, the sorbate concentration is very low, and the breakthrough curve is sensitive to even a modest contribution from external film resistance. In Figs. 3 and 4, in which the effects of feed concentration and flow rate are presented, respectively, only the dual resistance pore model was applied. There is some deviation from the model in some of the runs, particular in the initial region. It is possible that such a deviation may arise from axial dispersion, which is neglected in the theoretical model. However, in view of the good agreement observed in most of the runs, it seems more likely that these deviations arise simply from errors in the analysis. Such errors tend to be most pronounced at low water concentrations.

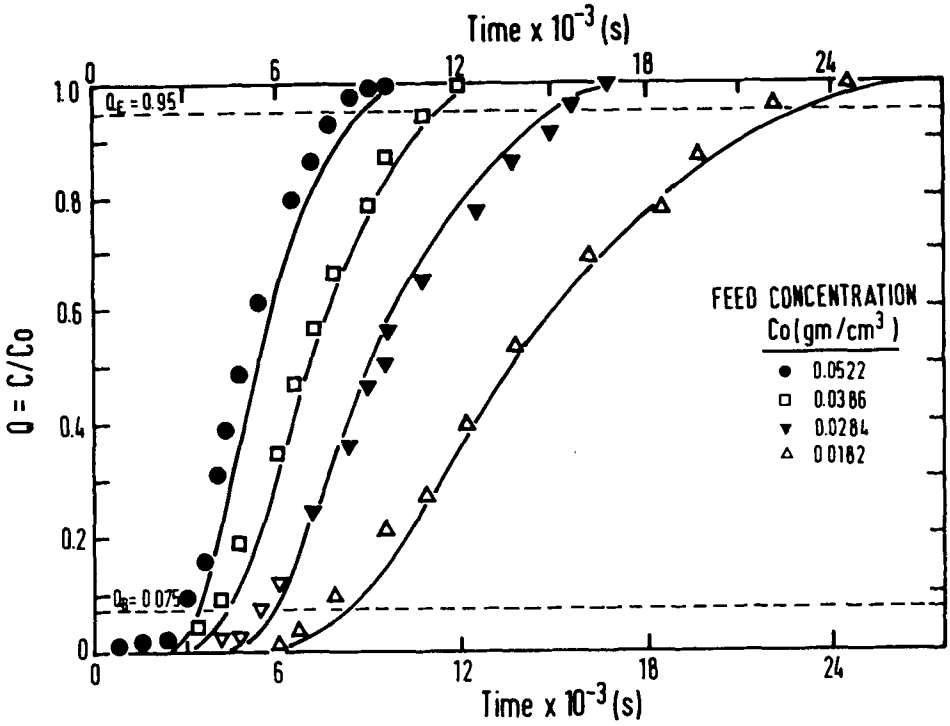

Fig. 3. Breakthrough curves: Effect of feed concentration. Lo=76.1 (cm); V=0.0822 (cm/s); Temp=24°C. (———): Predicted using dual resistance pore model.

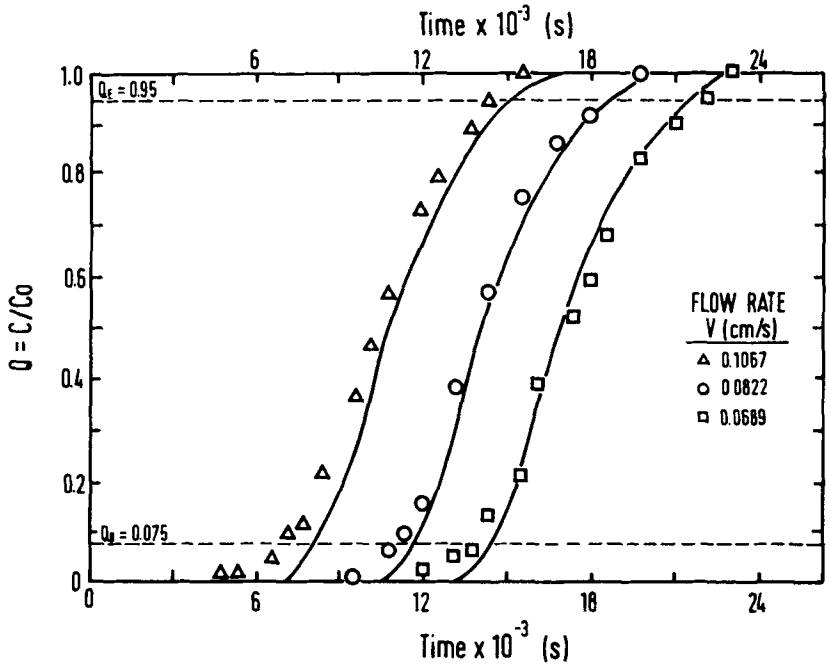

Fig. 4. Breakthrough curves: Effect of flow rate. Lo=152.2 (cm); Co= 0.0386 (g/cm^3); Temp=24°C. (———): Predicted using dual resistance pore model.

Table 1
Summary of Experimental Conditions and Parameters for Calculation of Breakthrough Curves Shown in Figs. 2–4[a]

Effect of Bed Length					
Bed length, cm	50.0	76.1	110.0	152.2	182.0
$\epsilon V \times 10^2$ cm/s	3.29	3.29	3.29	3.29	3.29
L_o/V, s	608	926	1338	1852	2214
$C_o, \times 10^2$ g/cm^3	3.86	3.86	3.86	3.86	3.86
N_p	1.887	2.874	4.153	5.748	6.872
$k_f \times 10^4$ cm/s	8.58	8.58	8.58	8.58	8.58
N_f	19.41	29.55	42.70	59.10	70.66
N_p/N_f	0.0972	0.0972	0.0972	0.0972	0.0972
Effect of Feed Concentration					
Bed length, cm	76.1	76.1	76.1	76.1	
$\epsilon V \times 10^2$ cm/s	3.29	3.29	3.29	3.29	
L_o/V, s	926	926	926	926	
$C_o, \times 10^2$ g/cm^3	1.82	2.84	3.86	5.22	
N_p	2.874	2.874	2.874	2.874	
$k_f \times 10^4$ cm/s	8.58	8.58	8.58	8.58	
N_f	20.15	20.15	20.15	20.15	
N_p/N_f	0.143	0.143	0.143	0.143	
Effect of Fluid Velocity					
Bed length, cm	152.2	152.2	152.2		
$\epsilon V \times 10^2$ cm/s	2.756	3.29	4.27		
L_o/V, s	2209	1852	1426		
$C_o, \times 10^2$ g/cm^3	3.86	3.86	3.86		
N_p	6.856	5.748	4.426		
k_f¼10^4 cm/s	7.83	8.58	9.85		
N_f	64.33	59.10	52.24		
N_p/N_f	0.107	0.0972	0.0847		

[a] $q_s = 0.176$ g/cm^3 (Capacity = 0.16 g/g from adsorption isotherm studies); $15\epsilon_p D_p/R_p^2 = 2.069 \times 10^{-3} s^{-1}$ where, $\epsilon_p = 0.33$ cm and $R_p = 0.121$ cm and $\epsilon = 0.4$.

Application of MTZ Model

The MTZ length, L_{MTZ}, and the fraction ability of the adsorbent within MTZ to still adsorb water and length of unused bed were determined from the experimental breakthrough curves under the independent variables examined. Table 2 summarizes the important operating condition, calculated MTZ heights, and percentage of bed saturation. The shape of the breakthrough curves is characterized by the value of f, which was found to be constant at 0.43 ± 0.02 for the molecular sieve used in this study.

The effect of fixed-bed height on the MTZ length is presented in Fig. 5. Over the bed height range (50–182 cm) investigated, the MTZ remained

Table 2
Principal Conditions and Results of Breakthrough Runs[a]

Bed height, cm	Bed weight, g	V× 10^2, cm/s	Feed concn.× 10^2, g/cm^3	t_B t_E ×10^{-3}, s		1−f	Equil. loading, g/g	MTZ height, cm	Bed satn., %
50.0	184	8.22	3.86	1.86	8.70	0.578	0.158	72.0	39.2
76.1	256	8.22	3.86	4.20	10.80	0.562	0.167	70.8	59.3
110.0	391	8.22	3.86	7.32	14.40	0.560	0.166	74.6	70.2
152.2	528	8.22	3.86	11.28	18.00	0.577	0.167	72.3	79.9
182.0	647	8.22	3.86	14.22	21.12	0.567	0.172	72.9	82.7
152.2	530	6.89	3.86	14.40	21.84	0.565	0.173	64.2	81.7
152.2	528	8.22	3.86	11.28	18.00	0.577	0.166	72.3	79.9
152.2	528	10.67	3.86	7.44	14.40	0.570	0.142	101.5	71.3
76.1	265	8.22	5.22	3.18	7.92	0.575	0.162	69.4	61.2
76.1	256	8.22	3.86	4.20	10.80	0.562	0.170	70.8	59.3
76.1	265	8.22	2.84	9.36	15.32	0.564	0.167	74.6	57.3
76.1	265	8.22	1.82	7.56	21.60	0.564	0.158	78.1	55.3
76.1	265	6.89	3.68	4.96	12.02	0.570	0.154	59.7	66.3
152.2	530	6.89	3.68	13.50	20.70	0.578	0.133	62.0	82.8
76.1	265	4.82	3.68	7.50	17.45	0.548	0.161	38.8	76.9

[a]Temp = 24°C

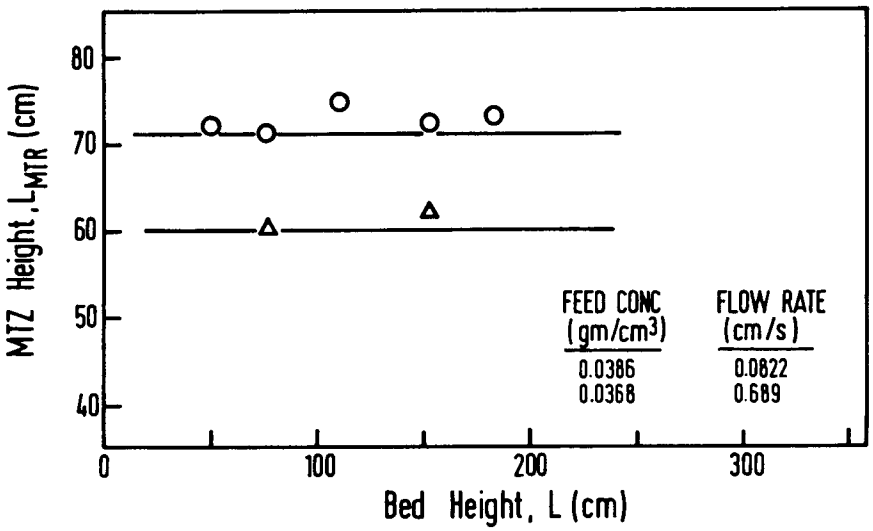

Fig. 5. Effect of bed height on height of mass-transfer zone. (○, △): Experimental data; (———): Predicted using Eq. (10).

fairly constant at 72±3 cm. The condition that the MTZ length be independent of bed height for the application of the Michaels method is thus satisfied. The MTZ length appeared to be sensitive to changes in the flow rate and lengthened as the flow rate increased, as shown in Fig. 6. The MTZ length increased with reduced feed water concentration, but the variation is moderate. These observations are reasonable, because one would expect the time for the development of the MTZ to be longer with increasing flow rate and/or reducing solute concentration. Therefore, these conditions will result in an increase in MTZ length.

Design Equation for Ethanol Dehydration

For the convenience of design calculations, the effects of the independent parameters, such as flow rate, feed solute concentration, and bed height, on the height of the MTZ, L_{MTZ}, may be related by combining Eqs. (5) or (6) with the theoretical model of Weber and Chakravorti (Eq. (1)). Based on Eq. (5), the empirical expression for the MTZ length is given in Eq. (10).

$$L_{MTZ} = 263L_oV/(4V + 0.264L_o + L_oC_o) \quad (10)$$

The above equation was developed based on Q_E at exhaustion and Q_B at breakthrough of 0.95 and 0.075, respectively. At the breakpoint, the fractional ability of the adsorbent within the MTZ for further adsorption was taken to be 0.43. The external mass transfer coefficient, k_f, was determined using Eq. (9).

The above expression represents the relative effect of water concentration and flow rate on the length of MTZ. The equation provides a rapid and fairly accurate prediction of the MTZ lengths at various operating conditions, as demonstrated in Figs. 5 and 6.

Since the adsorbent used in the MTZ length is only (1−f), the operating equilibrium capacity of the bed increases with increasing bed length. Figure 7 suggests that for effective use of bed capacity, a minimum of 5 to 6 times the MTZ length should be used.

CONCLUSION

The liquid phase dehydration of ethanol solutions using type 3A molecular sieves in fixed-bed adsorption column has been studied. Experimental breakthrough curves, obtained in fixed-bed adsorption studies, are well described by the dual resistance model of Weber and Chakravorti. The MTZ model was found to apply well to the dehydration system studied. A constant MTZ length independent of fixed-bed height was obtained. The shape of the breakthrough curve and the fraction ability of the adsorbent within the MTZ to still adsorb solute was found to be a constant. A simple design equation relating MTZ length to the various parameters has been developed by combining the theoretical model with the MTZ

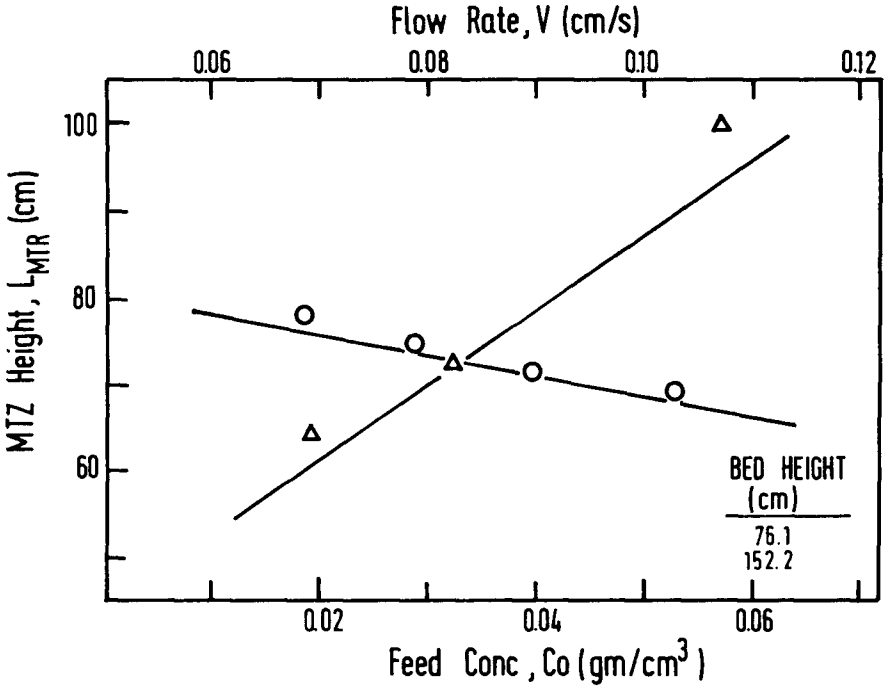

Fig. 6. Effect of feed concentration and flow rate on height of mass-transfer zone. (○, △): Experimental data; (———): Predicted using Eq. (10).

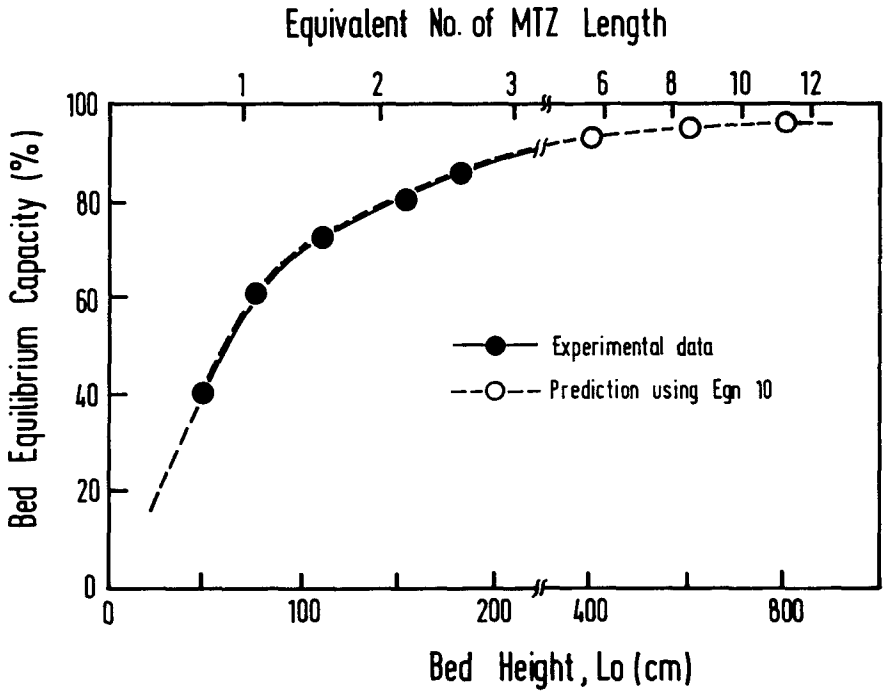

Fig. 7. Effect of bed height on the effective use of bed capacity. Data obtained at Co = 0.0386 (g/cm^3); V = 0.0822 (cm/s); Temp = 24°C.

model. This equation provides a simple approach to the design calculation for the dehydration system.

ACKNOWLEDGMENTS

The authors wish to thank D. M. Ruthven for his helpful suggestions and Lim Ai Lee for carrying out part of the experimental work. The financial support from the ASEAN Working Group on Management and Utilization of Food Waste Materials under the ASEAN-Australia Economic Cooperation Program is gratefully acknowledged.

REFERENCES

1. Teo, W. K. and Ruthven, D. M. (1986), *Ind. Eng. Chem. Process Des. Dev.* **25,** 17.
2. Ruthven, D. M. (1984), *Principles of adsorption and adsorption processes.* Wiley, New York.
3. Weber, T. W. and Chakravorti, R. K. (1974), *AIChE J.* **20,** 228.
4. Cooper, R. S. and Liberman, D. A. (1970), *Ind. Eng. Chem. Fund.* **9,** 620.
5. Lukchis, G. M. (1973), *Chem. Eng.* **6,** 111.
6. Michaels, A. S. (1952), *Ind. Eng. Chem.* **35,** 1296.
7. Treybal, R. E. (1980), Mass Transfer Operations, McGraw-Hill, New York.
8. Wakao, N. and Funazkri, T. (1978), *Chem. Eng. Sci.* **33,** 1375.